

Proceeding Paper

Dispersion Stability of MWCNTs Decorated with Ag Nanoparticles through Pulse-Reversed Current Electrodeposition Using a Deep Eutectic Solvent †

Ana T. S. C. Brandão ¹, Sabrina Rosoiu ², Renata Costa ¹, A. Fernando Silva ¹, Liana Anicai ^{2,3}, Carlos M. Pereira ^{1,*} and Marius Enachescu ^{2,4}

¹ Instituto de Ciências Moleculares IMS-CIQUP, Departamento de Química e Bioquímica, Faculdade de Ciências da Universidade do Porto, Rua do Campo Alegre, 687, 4169-007 Porto, Portugal; up200706627@edu.fc.up.pt (A.T.S.C.B.); renata.costa@fc.up.pt (R.C.); afssilva@fc.up.pt (A.F.S.)

² Center for Surface Science and Nanotechnology, University Polytechnica of Bucharest, Splaiul Independentei 313, 060042 Bucharest, Romania; sabrina.rosoiu@cssnt-upb.ro (S.R.); liana.anicai@cssnt-upb.ro (L.A.); marius.enachescu@cssnt-upb.ro (M.E.)

³ OLV Development SRL, Brasoveni 3, 023613 Bucharest, Romania

⁴ Academy of Romanian Scientists, Splaiul Independentei 54, 050094 Bucharest, Romania

* Correspondence: cmpereir@fc.up.pt

† Presented at the 3rd International Online-Conference on Nanomaterials, 25 April–10 May 2022;

Available online: <https://iocn2022.sciforum.net/>.



Citation: Brandão, A.T.S.C.; Rosoiu, S.; Costa, R.; Silva, A.F.; Anicai, L.; Pereira, C.M.; Enachescu, M. Dispersion Stability of MWCNTs Decorated with Ag Nanoparticles through Pulse-Reversed Current Electrodeposition Using a Deep Eutectic Solvent. *Mater. Proc.* **2022**, *9*, 29. <https://doi.org/10.3390/materproc2022009029>

Academic Editor: Antonio Di Bartolomeo

Published: 29 April 2022

Publisher's Note: MDPI stays neutral with regard to jurisdictional claims in published maps and institutional affiliations.



Copyright: © 2022 by the authors. Licensee MDPI, Basel, Switzerland. This article is an open access article distributed under the terms and conditions of the Creative Commons Attribution (CC BY) license (<https://creativecommons.org/licenses/by/4.0/>).

Abstract: Carbon nanotubes (CNTs) represent a unique class of nanomaterials with remarkable properties with a wide variety of applications in diverse scientific and technical domains. However, one of the many challenges still requiring improvement is undoubtedly their dispersion stability. The control of the dispersion stability of CNTs is a challenge due to the strong van der Waals forces that lead to their aggregation. Metallic nanoparticles (NPs), such as silver (AgNPs), in the presence of a capping agent, e.g., poly(N-vinyl pyrrolidone) (PVP 10), are recognized as having a key role in the increase of the stability of NP dispersions, and if incorporated in multi-walled CNTs (MWCNTs), may help surpass the MWCNTs' aggregation problem. The present work reports the enhancement of the stability of MWCNTs upon decoration by AgNPs, using an electrochemical method to generate the silver ions and promote the electrodeposition of silver. To validate the increase in stability of the Ag-decorated MWCNTs, two solvents were used, water and glyceline, a eutectic mixture of choline chloride and glycerol. The time stability of bare MWCNT and AgMWCNT nanofluids was characterized through dynamic light scattering (DLS) and ultraviolet–visible (UV–Vis) spectrophotometry. Compared to commercial MWCNTs, MWCNTs decorated with AgNPs presented a significant stability enhancement, in both water and glyceline. Glyceline also presented higher stability over time, with a retention of UV–Vis absorbance up to 97%, compared to 50% for water media. The DLS and turbidity experiments showed the same trend of MWCNTs' stability in water and glyceline. In both cases, the use of AgMWCNT materials improved the stability of the dispersions 25× in glyceline and 2.5× in water, when compared to the stability of bare MWCNT dispersions.

Keywords: stability; multi-walled carbon nanotubes; silver nanoparticles; pulse-reverse electrodeposition; deep eutectic solvent; electrochemical synthesis

1. Introduction

Carbon nanotubes (CNTs) were first reported by Oberlin et al. [1] and Iijima [2], and have been attracting the attention of the scientific community due to their unique mechanical, electrical and thermal properties. There are three distinctive types of CNTs, namely, single-walled (SWCNTs), double-walled (DWCNTs), and multi-walled carbon nanotubes (MWCNTs).

Even though CNTs are recognized as having promising applications, there are still fundamental problems that need to be solved, namely, the difficulty in obtaining uniform dispersions. Although good stability is a crucial property of a nanofluid in the maintenance of its enhanced properties, the hydrophobic nature of CNTs and the strong van der Waals interaction among adjacent CNTs can cause bundling or aggregation of CNTs and subsequently weak dispersion stability in fluids [3,4]. The dispersion of CNTs for various applications has already been reviewed [5,6].

The addition of surfactants has proven to be an effective way to enhance the dispersibility of CNTs [7–11]. However, the presence of surfactants may cause several new problems. For instance, when using CNTs dispersed in heat transfer fluids [12], the addition of surfactants can contaminate the heat transfer media, and furthermore, surfactants tend to produce foam when heated and deteriorate the system. In addition, the surfactant molecules attach to the surface of the CNTs, enlarging the thermal resistance between the CNT and the base fluid, which limits the enhancement of the effective thermal conductivity.

To fully exploit the superior characteristics of CNTs and to extend the range of applications of CNT-containing nanofluids, it is essential to use a well thought-through method to prepare nanofluids without adding surfactants.

Another possible mechanism to stabilize CNT dispersion is the decoration of CNTs with metal nanoparticles (NPs) [13,14]. Metal nanoparticles (NPs) have higher electrochemical activity, and their dispersion in water is expected to be more stable than CNTs [15]. CNTs are ideal templates to immobilize a variety of nanoparticles, attracting increasing attention from researchers interested in using CNT composites in diverse applications such as batteries, fuel cells, sensors, catalysis, hydrogen storage and heat transfer. Various metals (i.e., Ag, Au and Pt) have been studied for the decoration of CNTs [16–19]. Ag nanoparticles (AgNPs) have received particular attention [14,20–26] due to their high conductivity, which leads to their ability to improve the electrical conductivity of CNTs. The potential of AgNPs has already been demonstrated in the development of electrode materials with innovative properties [18], biosensors [27] and antibacterial agents [14,28].

The electrochemical synthesis of AgNPs in aqueous/non-aqueous systems is a cheap and effective way to control the size of the NPs [25,27–29]. However, aqueous systems present limitations such as poor dispersion and low electrochemical stability [29]. On the other hand, ionic liquids (ILs) may provide some advantages that can make them more suitable for energy storage applications. Nevertheless, ILs present high production and purification costs, making them less competitive than traditional solvents. To beat this obstacle, Abbott et al. [30,31] developed a eutectic mixture of a quaternary ammonium salt (choline chloride) with amides and glycols (such as ethylene glycol, glycerol, etc.), as hydrogen bond donors (HBDs), creating a cheaper and more eco-friendly alternative to the conventional ILs. These liquids are known as deep eutectic solvents (DESs), and are categorized as IL analogues [32].

Cojocaru et al. [26] proposed for the first time the electrochemical synthesis of AgNPs involving a choline chloride–glycerol-based DES using the pulse-reversed current technique, with poly(N-vinyl pyrrolidone) (PVP) as a capping agent to prevent agglomeration and to control the growth of the AgNPs [33]. The electrochemical synthesis of AgNPs on the surface of MWCNTs was successfully achieved by Brandão et al. [34], through pulse-reverse electrodeposition in a choline chloride–glycerol eutectic mixture as electrolyte. The obtained composites presented a significant enhancement in their electrochemical performance, as demonstrated by the increase in electrode stability and specific capacitance.

Many publications have studied and identified the various factors that influence the stability of nanofluids, such as particle volume concentration [35], particle size [36], shape [37], temperature [38], pH [38], material [39] and fluid type [40].

Dynamic light scattering (DLS) and ultraviolet-visible (UV–Vis) spectrophotometry are fast and easy-to-operate techniques for particle characterization, especially for colloidal suspensions [41,42]. There are several advantages of DLS [43,44] and UV–Vis [45–47] techniques, including simplicity, sensitivity and selectivity to NPs, and short time of

measurement. Therefore, these techniques are increasingly used for the characterization of NPs in many fields of science and industry [43,48].

Both techniques can provide essential time-dependent dispersion information from DLS and UV–Vis spectra during the dispersion process to quantify suspension quality and understand dispersion mechanisms.

The theory and mathematical bases that allow interpretation of UV–Vis radiation with nanoparticles are well established and can be found in the literature [49]. Nanoparticles have optical properties that are very sensitive to size, shape, agglomeration and concentration changes [49].

DLS measures the light scattered from a laser that passes through a colloid. Next, the modulation of the scattered light intensity as a function of time is analysed, and the hydrodynamic size of particles can be determined [50].

In this work, the stability of AgMWCNT composites in glyceline and water was investigated. The morphology of the AgMWCNT composites was characterized by SEM, while the stability of the AgMWCNT-based fluids was studied by DLS and UV–Vis.

To the best of the authors' knowledge, this is the first time that the stability of MWCNTs decorated by AgNPs, dispersed in a choline chloride–glycerol eutectic mixture has been studied. The same eutectic was used for synthesising the AgNPs and as dispersant medium to improve the surface wettability of the composite material by the solvent.

2. Materials and Methods

2.1. Chemicals and Preparation of DES

Choline chloride (ChCl, Sigma Aldrich, 99%, Darmstadt, Germany), glycerol (Sigma Aldrich, 99%, Darmstadt, Germany) and poly(N-vinyl pyrrolidone) (PVP 10, Sigma Aldrich, 99%, Darmstadt, Germany) were used as received.

The eutectic mixture was formulated by mixing and heating at 60 °C the ChCl with glycerol, as HBDs, in the molar ratio of 1:2, until a homogeneous and clear liquid was formed. This liquid will be referred to from here on as glyceline.

2.2. Electrochemical AgNP Synthesis

The experimental procedure for the synthesis of AgMWCNT composites has already been presented in detail by Brandão et al. [34]. Briefly, poly(N-vinyl pyrrolidone) (PVP 10, Sigma Aldrich, Darmstadt, Germany) was added to glyceline to prepare a 5 g L⁻¹ solution and stirred until its complete dissolution. Commercial MWCNTs (Sigma Aldrich, 99%, Darmstadt, Germany) were dispersed in this 30 mL mixture, using a 50 mL glass beaker, and were processed in an ultrasonic bath with a peak ultrasonic power of 360 W (Sonica S3, Soltec, Milan, Italy) for 30 min. The electrochemical deposition was performed in a pulse-reverse current mode using a pulse-reverse current power supply (pe 86CB 3HE, Plating Electronic GmbH, Sexau, Germany) at room temperature and a two-electrode cell configuration. Both electrodes were composed of Ag wires with an exposed area of approximately 5 cm².

Several studies were performed with different applied anodic and cathodic currents, and different on- (t_{ON}) and off-times (t_{OFF}). The studied parameters are presented in Table 1.

Table 1. Parameters for the electrodeposition process of AgMWCNTs. Data from Brandão et al. [34] **.

Sample	t_{ON} (Anodic and Cathodic)/ms	t_{OFF}/ms	Current (Anodic and Cathodic) (i_{ON})/mA	Overall Time/min
A	100		±100	30
B	100	200	±100	60
C	200		±100	60
D*	100		±100	60

* Ultrasound was used during electrodeposition. ** Reprinted from Characterization and electrochemical studies of MWCNTs decorated with Ag nanoparticles through pulse reversed current electrodeposition using a deep eutectic solvent for energy storage applications, Pages No. 342–359, Copyright (2021), with permission from Elsevier [34].

The pulse-reverse electrodeposition method begins with the application of an anodic current (positive pulse) in which the Ag wires start to dissolve, releasing Ag^+ to the glyceline media, followed by an OFF time. Ultimately, a cathodic current (negative pulse) is applied in which the Ag^+ is reduced and the Ag nuclei produced are trapped on the MWCNT's surface. All electrodepositions were performed under magnetic stirring; ultrasound was also used during electrodeposition to understand its effect.

2.3. Morphological Characterization

The morphology and composition of the electrochemically prepared AgMWCNT samples were analysed by scanning electron microscopy (SEM) associated with energy-dispersive X-ray (EDX) analysis (Hitachi SU 8230 equipment, Krefeld, Germany), after separation by centrifugation and multiple-step rinsing.

The average AgNP size was established through particle-size distribution (PSD) analysis, using the scientific image analysis software Image J (version, 1.53), through the analysis of the SEM micrographs. In the Image J software, a band pass filter was applied, followed by thresholding. The histogram data plot was developed using Origin 2016, followed by the Gaussian function, obtaining the average NP size and the standard deviation. The polydispersity (PD) value obtained for the various samples was calculated using Equation (1).

$$\text{PD} = \frac{\text{Standard deviation}}{\text{Average NP size}} \times 100 \quad (1)$$

2.4. Stability Characterization

To determine the stability of the AgMWCNTs, the composites were left in suspension (in glyceline and water— 0.4 mg cm^{-3}) without agitation. Visual observation was conducted to detect suspended particles or sediment. In addition to visual observation, DLS and a UV-Vis spectrophotometer were used to quantify changes in light dispersion induced by the dispersed nanomaterials.

Dynamic light scattering (DLS, W130i, Avid Nano, High Wycombe, UK) was used to determine the standard deviation throughout the time of analysis. The samples were analysed throughout the experimental period, from 0 to 120 h, to study the dispersion stability of the material in glyceline and water, as reference. All samples were dispersed in glyceline and water to suitable concentrations and analysed in triplicate. The refractive index of the glyceline analysed in this work was 1.3331, and the viscosity was 497 Cp at 20°C [51].

The absorption spectra of MWCNTs and AgMWCNTs in glyceline and water were also examined over the wavelength of 200 to 600 nm, using an ultraviolet-visible (UV-Vis) spectrophotometer (T60, PG instruments, Leicestershire, UK). The samples were analysed throughout the experimental period, from 0 to 120 h. The absorbance measured over time was used to measure the stability of the suspensions.

The turbidity of the carbon samples was measured using a Hach 2100Q Portable Turbidimeter (Hach, Ames, IA, USA) for MWCNTs and AgMWCNTs (Sample D).

3. Results

3.1. Stability of MWCNT and AgMWCNT Composites' Dispersion in Glyceline and Water Media

The monitoring of the stability of the dispersion of the AgMWCNT composites in glyceline media is also of significant importance since the electrodeposition process is dependent on the degree of aggregation of the MWCNTs. It has been proved that the decoration of CNTs with AgNPs can enhance the stability of the CNTs' dispersion, reducing surface energy and van der Waals forces between them [25].

3.1.1. Scanning Electron Microscopy and Polydispersity Determination

Figure 1 presents the SEM images of the commercial MWCNTs and AgMWCNT composites. As previously reported by Brandão et al. [34], the AgNPs were successfully

attached to the MWCNTs' walls (Figure 1b–e), where it is possible to see the morphological differences when using different electrodeposition parameters, with Sample C (Figure 1b) and Sample D (Figure 1e) presenting agglomerated AgNPs, where the increase of the time of the applied current (Sample C: 100 ms to 200 ms) and ultrasound (Sample D) are the key parameters for this phenomenon.

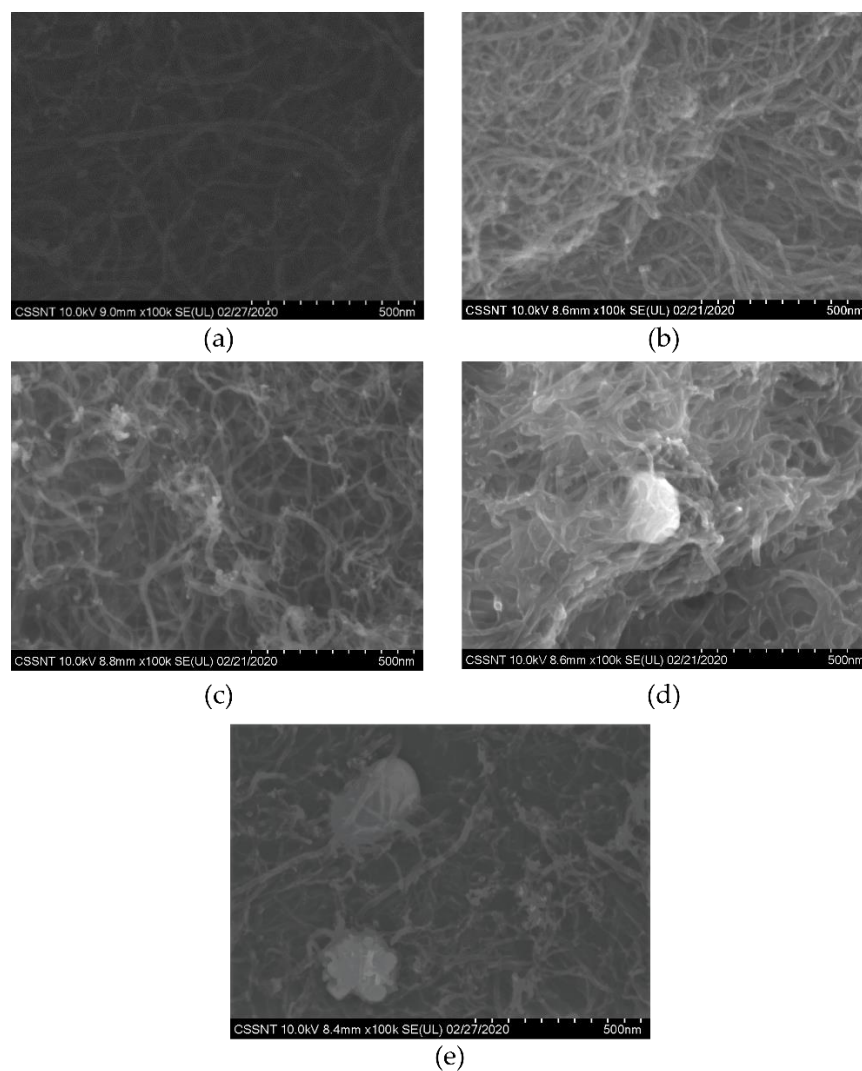


Figure 1. SEM analysis of commercial MWCNTs (a) and Samples A to D (b–e) of AgMWCNT composites at $\times 100k$.

The polydispersity (PD) determination from particle-size distribution (PSD) analysis was obtained through the average NPs diameter and the standard deviation of a static SEM image (Figure 1), not taking into consideration the possible agglomeration of the material.

The average NPs diameter and the PD were calculated using the Image J analysis and applying the PSD method; the results are presented in Table 2.

Table 2. Average diameter and PD obtained through particle-size distribution of the AgNPs of the various AgMWCNT composites, after SEM analysis through the Image J software.

Samples	AgNP Size (nm)	Polydispersity (%)
A	12 ± 5	40
B	16 ± 4	25
C	33 ± 6	19
D	46 ± 7	15

The PD calculation obtained through SEM image analysis cannot be used as a comparison to the DLS analysis, since SEM images do not reveal details about the dynamics and stability of the solutions. The PD values in relation to the PSD results indicate values up to 40%. This method presents the advantage of allowing the determination of the average AgNP size. A higher AgNP size in Sample D was already obtained by Brandão et al. [34], when ultrasound was used. Even though ultrasound leads to a decrease in MWCNT aggregation and an increase in mass transfer and greater available area for AgNPs, a significant increase in size of AgNPs is observable. The justification for this AgNP size increase may be associated with the fact that ultrasounds may accelerate the rate of AgNP formation, due to the increase in temperature causing faster nuclei growth [52].

3.1.2. UV–Vis Analysis

The UV–Vis spectrum is an effective method to quantitatively evaluate CNT [53,54] and AgNP [55] dispersion at the nanoscale. Individual CNTs are more absorptive in the UV–Vis region [56], while bundled CNTs are barely active in this range. UV–Vis spectroscopy has been successfully employed to investigate the dispersion behaviour of MWCNTs and AgMWCNT composites in both glyceline and water.

Figure 2a,b present the UV–Vis absorption of MWCNT and AgMWCNT (Samples A to D) suspensions in glyceline and water, respectively, at the initial time ($t = 0$ h). As can be seen in Figure 2a,b, the absorption spectrum of MWCNTs shows predominant peaks at 253 nm and 252 nm for glyceline and water, respectively, which is in good agreement with the literature [57,58]. This peak may be associated with the π – π^* transition of the aromatic C–C bonds [56–58]. The glyceline medium presents an increase in absorbance ($\times 2$) compared to water.

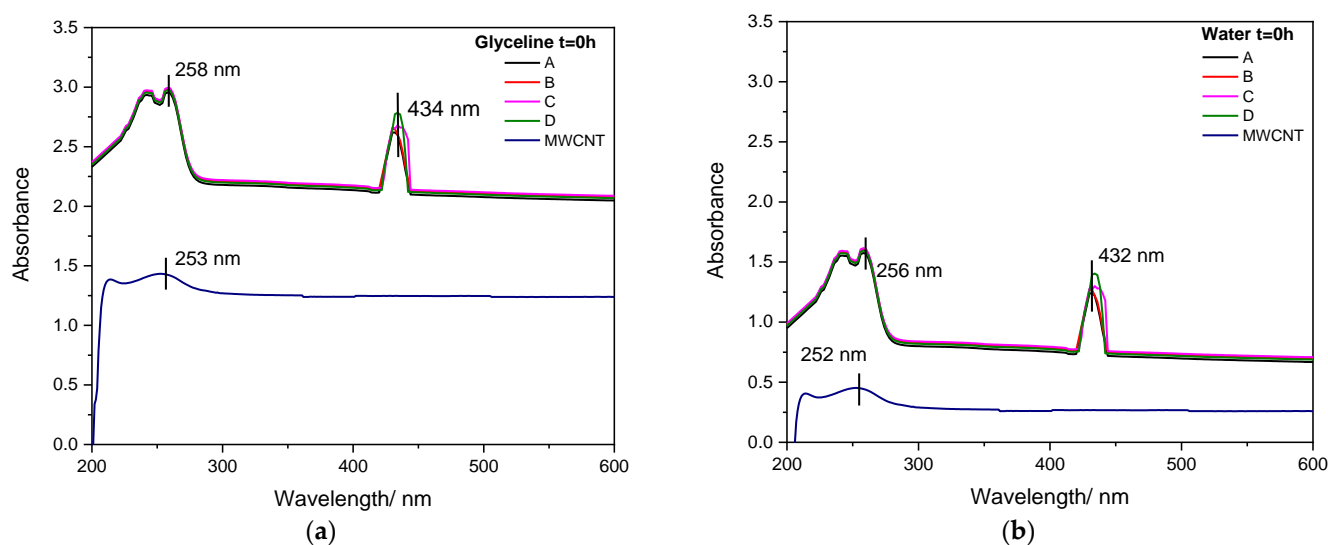


Figure 2. UV–Vis absorption spectra of MWCNT and AgMWCNT composite dispersion (0.4 mg cm^{-3}) in glyceline (a) and water (b) at $t = 0$ h, at room temperature.

There are two distinct peaks in the absorption spectra of AgMWCNTs. The peaks at 258 nm and 256 nm (for glyceline and water, respectively) are similar to those presented in the MWCNTs spectra. The additional peaks at 434 nm and 432 nm (for glyceline and water, respectively) are attributable to the surface plasmon resonance of AgNPs, which also confirms the successful incorporation of AgNPs, as established by several authors [25,59–62].

The UV–Vis spectra of AgNPs correlates with the size and shape of AgNPs [61,62], in which spherical AgNPs exhibit a single absorption peak. The single peak around 430 nm associated with the AgNPs in the AgMWCNTs' spectra shows that the AgNPs have a spherical shape, which agrees with the analysis of the SEM/STEM images. According to Chen et al. [63], with the increase in the AgNPs size, the peak broadens, which is in good

agreement with the present results, since Samples C and D present bigger NP size and the associated broadening of the absorption peak.

The translation of the spectra, when comparing the UV-Vis spectra of MWCNT dispersions and those of Ag-decorated MWCNTs is related to the increased stability of decorated MWCNT dispersions, which induce much greater light dispersion and therefore an increased baseline absorption [22,64].

The time dependence of the UV-absorption peaks of MWCNTs and AgMWCNTs in both glyceline and water were used to evaluate the dispersion stability (UV-Vis absorption spectra for the different periods are not shown here). It is widely accepted that absorption intensity is proportional to the concentration of individual CNTs, and small bundles dispersed in the suspension [53]. Further, MWCNT sedimentation will reduce the light scattering and can therefore be used to evaluate dispersion stability. To compare the sedimentation rate of the MWCNT dispersions under study, the UV-Vis spectra were normalized, and Figure 3a,b shows the retention of the initial absorbance of the MWCNTs' and AgMWCNTs' UV absorption peaks of the different samples measured at different times, in glyceline and water, respectively, with reference to the UV-Vis peak associated with the MWCNTs (represented in Figure 2a,b).

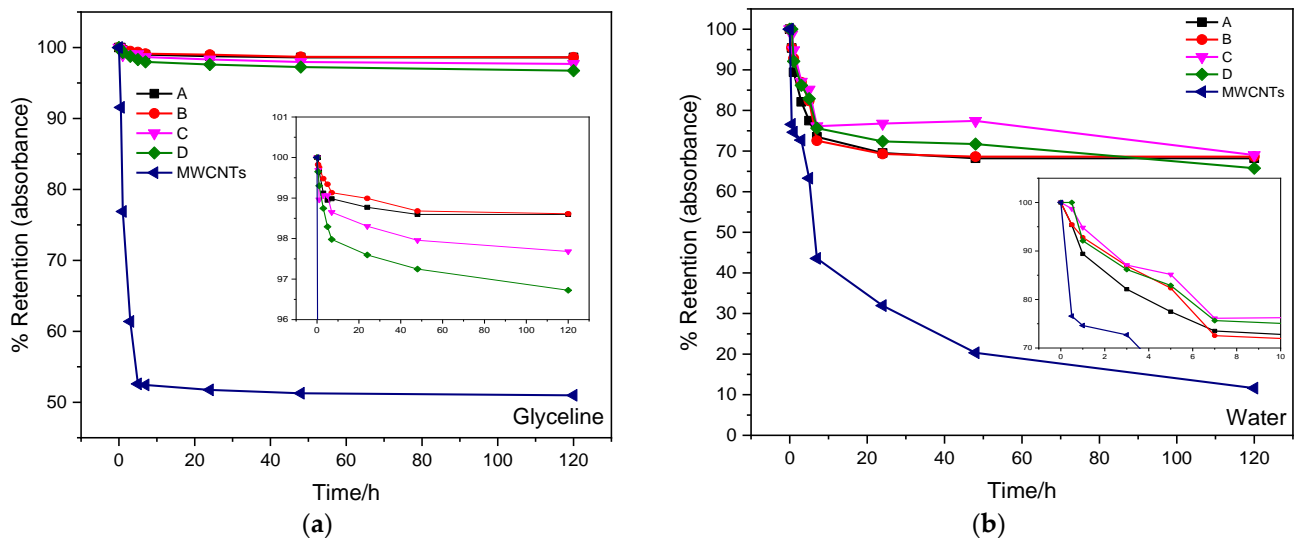


Figure 3. Time dependence of UV-Vis absorption at 253 nm and 252 nm (glyceline and water, respectively) of different samples in glyceline (a) and water (b) media, at room temperature (dispersions prepared from 0.4 mg of MWCNTs or AgMWCNTs in 1 cm³ of each solvent).

All samples show a decrease in the absorption peak intensity with time, due to the re-aggregation of individual and small bundles of MWCNTs and AgMWCNTs [65]. The glyceline medium presented better dispersion stability compared to water, with small variance throughout time, and absorbance retention up to 50%; in water medium the absorbance retention was up to 10% with the MWCNT dispersion.

A closer look at the results shows that two stages can be observed in the sedimentation process, with a fast decrease in absorbance retention in the early stage of the study. The shift seems to occur after 10 h in glyceline and 3 h in water, as can be observed in the in-set graphs in Figure 3.

In glyceline, the AgMWCNT samples showed greater stability over time (retaining around 98% of the initial absorbance) and remaining constant after 5 h. In water, in the first 5 h, there was a significant decrease in the absorbance (retaining around 70% of the initial absorbance value) for all the AgMWCNT samples, with a low value of absorbance compared to the samples in glyceline media.

Data from Figure 3a,b was analysed to extract the kinetic parameters for sedimentation of the MWCNTs and decorated MWCNTs in glyceline and water. As reported in the

literature [66], the sedimentation of the MWCNTs can be described by an exponential decay fitting function:

$$y = A_1 e^{(-kt)} + y_0$$

where k is the rate constant of sedimentation (h^{-1}), A_1 is the pre-exponential factor and y_0 is the value of y when $t = t_0$. The fitting parameters are presented in Table 3.

Table 3. Fitting parameters for the analysis of the MWCNTs sedimentation kinetics by an exponential decay function.

	Sample	$y_0/\text{a.u.}$	$A_1/\text{a.u.}$	k/h^{-1}	t_{half}/h	R^2
Glyceline	A	2.812 ± 0.002	0.039 ± 0.003	0.314 ± 0.006	2.5 ± 0.5	0.954
	B	2.843 ± 0.002	0.035 ± 0.002	0.15 ± 0.04	4.8 ± 1.1	0.949
	C	2.829 ± 0.005	0.050 ± 0.007	0.114 ± 0.005	6.5 ± 3.1	0.839
	D	2.788 ± 0.004	0.077 ± 0.006	0.17 ± 0.04	4.1 ± 0.8	0.948
	MWCNTs	0.81 ± 0.01	0.596 ± 0.002	0.33 ± 0.06	2.3 ± 0.1	0.991
Water	A	1.04 ± 0.02	0.46 ± 0.02	0.28 ± 0.02	2.5 ± 0.2	0.990
	B	1.05 ± 0.02	0.48 ± 0.03	0.21 ± 0.03	3.6 ± 0.5	0.975
	C	1.16 ± 0.04	0.41 ± 0.04	0.24 ± 0.07	3.1 ± 0.9	0.914
	D	1.11 ± 0.01	0.45 ± 0.08	0.25 ± 0.07	2.6 ± 0.6	0.932
	MWCNTs	0.30 ± 0.06	0.67 ± 0.08	0.33 ± 0.04	2.1 ± 2.1	0.986

a.u.—arbitrary units.

Bare MWCNTs present the worst stability in both media, which can be easily identified by the lower half-life time (t_{half}), showing that the incorporation of AgNPs helps the stability of the MWCNTs in suspension. According to Kausar et al. [67], that may be due to the reduction of the van der Waals forces among CNTs by AgNPs. The positive effect of AgNPs on the MWCNTs' dispersion led to them forming fewer aggregates or entangled bundles. Although the decoration of MWCNTs with AgNPs leads to an improvement in overall stability, it is notable that not all the decorated MWCNTs behave the same way, as can be seen with Sample C presenting a higher half-life time.

The results show that glyceline presents better dispersion stability when compared to water. This outcome is corroborated by Zaib et al. [68], who studied the dispersion of SWCNTs in an aqueous system containing glyceline and observed that a high concentration of glyceline in water ($\geq 80\%$) leads to SWCNTs uniformly dispersed.

3.1.3. Dynamic Light Scattering Analysis

DLS is a dynamic measurement, extremely sensitive to the dispersion/aggregation behaviour of the particles in solution [69]. It was used to study the stability of the various samples throughout time, in glyceline and water, to understand the effect of the DES on the stability of the AgMWCNT composites.

Figure 4 presents the evolution of the hydrodynamic diameter (Figure 4a) and the polydispersity (Figure 4b) over time, up to 120 h, for MWCNTs and Sample D. The comparison of the evolution of the hydrodynamic diameter over time for both samples shows that Sample D dispersed in glyceline presents better stability over time, compared to water media. Taking into consideration the polydispersity evolution over time, both samples present lower values of polydispersity in glyceline (up to 15%), compared to 70% of polydispersity of MWCNTs dispersed in water.

DLS analysis enables measurement of the hydrodynamic size of particles—in this case, MWCNTs and attached AgNPs. However, the geometric characteristics of the carbon nanotubes, which are far from being spherical particles, do not allow a realistic value for the hydrodynamic diameter to be obtained. Nevertheless, the hydrodynamic equivalent diameter reported by DLS analysis does generate a realistic picture of the evolution of the particles' dispersion of the light and therefore of the sample stability [65]. Both hydrodynamic equivalent diameter and polydispersity show that samples prepared in glyceline are more stable than those in water. However, the high light dispersion and inadequate

data modelling also contribute to the high PD values, which can lead to misinterpretations. Therefore, we evaluated the standard deviation of the DLS data. The evolution of the standard deviation throughout time is presented in Figure 5, for both glyceline and water (Figures 5a and 5b, respectively).

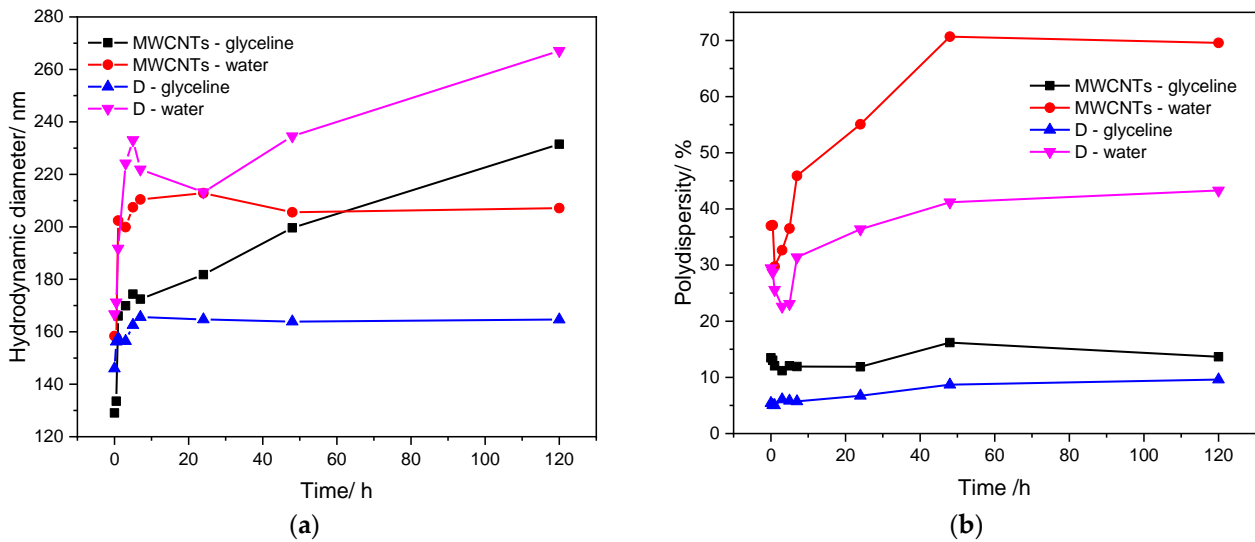


Figure 4. Hydrodynamic diameter (a) and polydispersity (b) evolution over time for MWCNTs and Sample D dispersed in glyceline and water media.

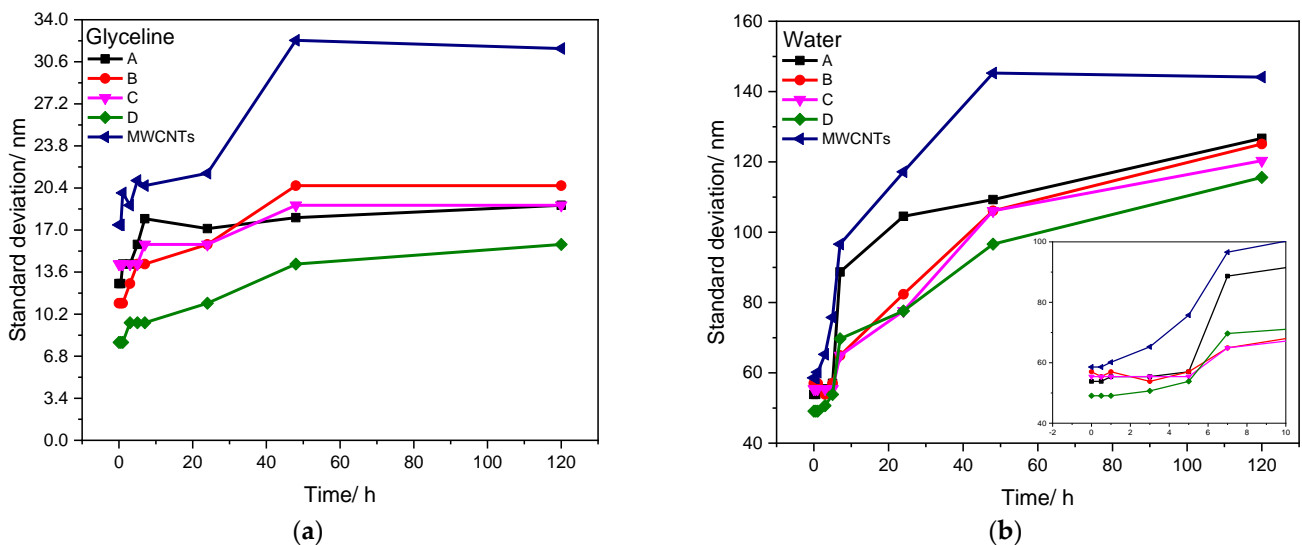


Figure 5. Standard deviation obtained through DLS analysis throughout time (0–120 h) for glyceline (a) and water (b) media, at room temperature, with 0.4 mg cm^{-3} of MWCNT and AgMWCNT composite samples.

The analysis of the stability of the samples through DLS analysis shows a very notable difference between glyceline and water media. Glyceline presents low values of standard deviation, with higher values for commercial MWCNTs. The AgMWCNT samples present standard deviation values below 40 nm, with stable values throughout time, indicating good stability of the media.

The same does not happen in water. The increase of standard deviation throughout time is highly accentuated, with higher values for commercial MWCNTs, with all AgMWCNT composite samples reaching values from 50 nm to 140 nm, indicating that the suspension tends to agglomerate over time. This shows that glyceline is an excellent

medium for the dispersion of MWCNTs and AgMWCNT composites, due mostly to the viscosity of the system. Brandão et al. [51] previously studied the physicochemical properties of the glyceline dispersions containing MWCNTs and AgMWCNTs, showing that glyceline presents a viscosity value $500\times$ higher than water (at $20\text{ }^{\circ}\text{C}$). However, an interesting trend was found in which the presence of MWCNTs in a glyceline dispersion decreases its viscosity; the same effect is not shown in water. On the other hand, there is a slight increase in the dispersion viscosity with the introduction of AgNPs on the surface of MWCNTs, for both glyceline and water. It is also important to refer that the presence of AgNPs helps to increase the stability of the AgMWCNT composites in both media. This may be due to the protective role [70] of PVP used for AgNPs synthesis, as it retards the growth and agglomeration of NPs by steric effect [71] and obtains a narrow size distribution of metal NPs, as presented previously by Brandão et al. [34].

3.1.4. Turbidity Analysis

The turbidity analysis was based on a comparison of the light intensity spread over the sample under defined conditions, with the light intensity spread by suspension considered standard. Therefore, the greater the intensity of the spread light, the greater the turbidity in the sample under analysis [72]. The turbidity test was performed for MWCNT and AgMWCNT (sample D) dispersions in glyceline and water to determine the amount of carbon material suspended in the fluid throughout time (up to 120 h); the results are presented in Figure 6.

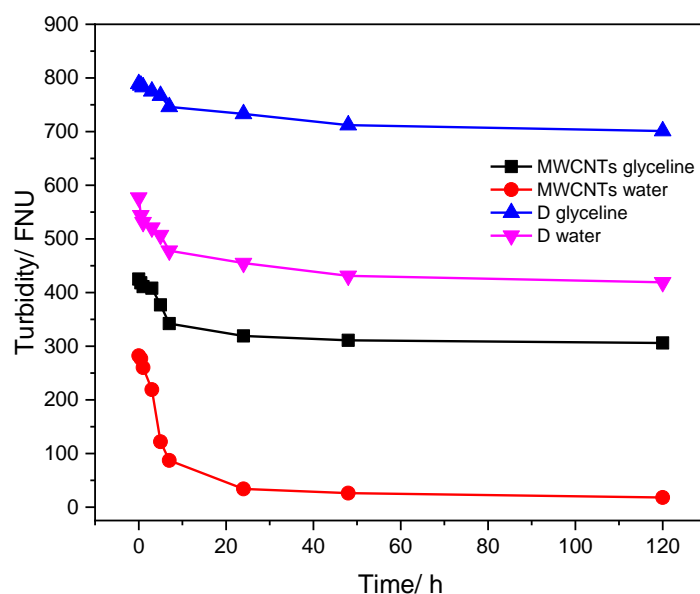


Figure 6. Turbidity studies over time for MWCNTs and Sample D dispersed in glyceline and water.

As can be observed in Figure 6, the turbidity of the carbon materials dispersed in both media decreases over time. However, Sample D presents the best stability over time in both media, as observed through the UV–Vis and DLS analysis. The higher variation was seen in the first 10 h of the study, for all samples.

3.1.5. Visual Analysis

Figure 7 presents the visual analysis of the MWCNT and AgMWCNT dispersions in both glyceline and water. A stable dispersion in glyceline was observed for all samples, while in water carbon materials were visible as sediment at the bottom. In glyceline, the colour of the dispersion remained almost constant, while in water it could be seen that the dispersion (even for $t = 0\text{ h}$) was not as good as in glyceline and there was a net difference at $t = 120\text{ h}$.

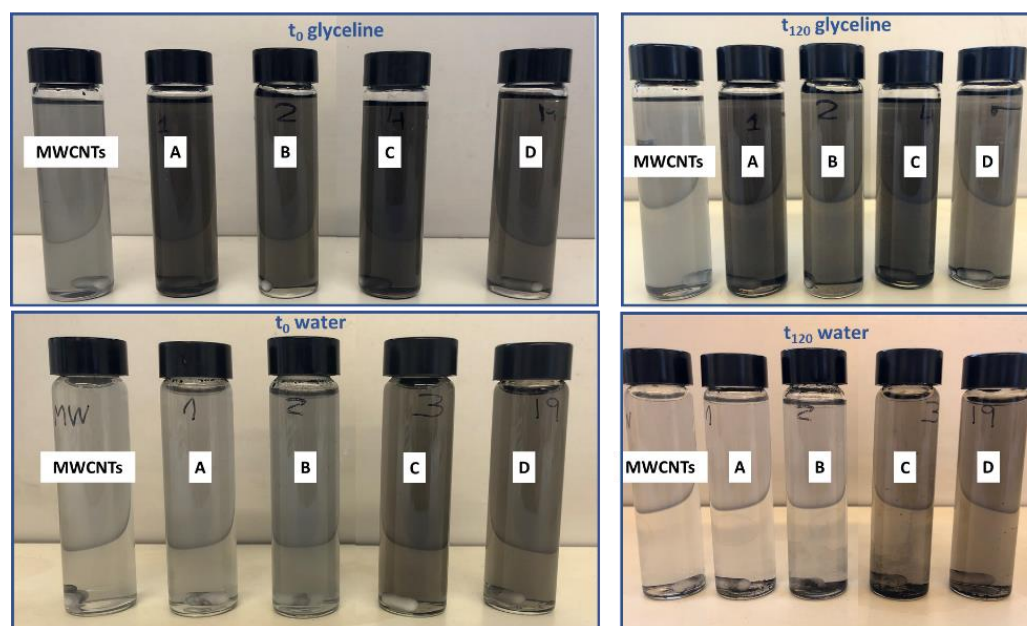


Figure 7. Physical observation of MWCNT and AgMWCNT dispersions in glyceline and water at $t = 0$ h (after sonication) and $t = 120$ h.

The visual observations of the samples over time in different media were consistent with the results obtained from the DLS and UV–Vis analysis, showing higher stability using glyceline as a dispersant medium. The viscosity of the medium is intimately related to the stability over time, with glyceline presenting a higher viscosity.

4. Conclusions

Stability tests were performed for dispersions of MWCNTs and AgMWCNT composites in glyceline and water. The DLS and turbidity measurements confirmed the results from the analysis of UV–Vis absorption at 253 nm and 252 nm (glyceline and water, respectively); however, the UV–Vis absorption measurements revealed more details of the stability of MWCNTs and Ag-decorated MWCNTs in glyceline and water.

Both DLS and UV–Vis analysis showed that the incorporation of AgNPs on MWCNTs' surface increases the stability of the composite in both studied media. A stable dispersion of MWCNTs, even after 120 h, can be prepared in glyceline after the MWCNTs have been decorated with AgNPs, while in water, MWCNT dispersions are significantly less stable. AgNPs presented a positive effect on the MWCNTs' stability since it leads to the formation of fewer carbon aggregates or entangled bundles.

Author Contributions: Conceptualization: A.T.S.C.B. and C.M.P.; methodology: A.T.S.C.B. and C.M.P.; formal analysis: A.T.S.C.B. and C.M.P.; investigation: A.T.S.C.B., R.C., S.R. and C.M.P.; writing—original draft: A.T.S.C.B.; writing—review and editing: A.T.S.C.B., S.R., R.C., L.A., M.E. and C.M.P.; supervision: A.F.S., L.A., M.E. and C.M.P.; resources: M.E. and C.M.P.; funding acquisition: M.E. and C.M.P. All authors have read and agreed to the published version of the manuscript.

Funding: This work was financially supported by the FCT under Research Grant UIDB/00081/2021–CIQUP, LA/P/0056/2020 (IMS) and H2Innovate NORTE-01-0145-FEDER-000076. This work was partially supported by an STSM Grant from the COST Action CA15107 MultiComp, supported by the COST Association (European Cooperation in Science and Technology). This work was supported by Romanian Ministry of Research, Innovation and Digitalization, Romania, under JINR-RO Project no. 91 Code Theme 04-4-1133-2018/2023, Grant no. 37/2021, ECSEL-H2020 projects: Pin3S Contract no. 10/1.1.3H/03.04.2020 Code MySMIS 135127 and BEYOND5 Contract no. 12/1.1.3H/31.07.2020 Code MySMIS 136877. Ana Brandão thanks the scholarship awarded by FCT with reference 2021.04783.BD, SCANSCI—equipamentos de laboratório for the financial support given to the PhD program and

the IL4Energy project. Renata Costa thanks FCT for funding through program DL 57/2016–Norma transitória (SFRH/BPD/89752/2012).

Institutional Review Board Statement: Not applicable.

Informed Consent Statement: Not applicable.

Data Availability Statement: Not applicable.

Conflicts of Interest: The authors declare no conflict of interest.

References

1. Oberlin, A.; Endo, M.; Koyama, T. Filamentous growth of carbon through benzene decomposition. *J. Cryst. Growth* **1976**, *32*, 335–349. [[CrossRef](#)]
2. Iijima, S. Helical microtubules of graphitic carbon. *Nature* **1991**, *354*, 56. [[CrossRef](#)]
3. Yang, S.-Y.; Ma, C.-C.M.; Teng, C.-C.; Huang, Y.-W.; Liao, S.-H.; Huang, Y.-L.; Tien, H.-W.; Lee, T.-M.; Chiou, K.-C. Effect of functionalized carbon nanotubes on the thermal conductivity of epoxy composites. *Carbon N. Y.* **2010**, *48*, 592–603. [[CrossRef](#)]
4. Zhang, M.; Su, L.; Mao, L. Surfactant functionalization of carbon nanotubes (CNTs) for layer-by-layer assembling of CNT multi-layer films and fabrication of gold nanoparticle/CNT nanohybrid. *Carbon N. Y.* **2006**, *44*, 276–283. [[CrossRef](#)]
5. Manzetti, S.; Gabriel, J.-C.P. Methods for dispersing carbon nanotubes for nanotechnology applications: Liquid nanocrystals, suspensions, polyelectrolytes, colloids and organization control. *Int. Nano Lett.* **2019**, *9*, 31–49. [[CrossRef](#)]
6. Njuguna, J.; Vanli, O.A.; Liang, R. A Review of Spectral Methods for Dispersion Characterization of Carbon Nanotubes in Aqueous Suspensions. *J. Spectrosc.* **2015**, *2015*, 463156. [[CrossRef](#)]
7. Tkalya, E.E.; Ghislandi, M.; de With, G.; Koning, C.E. The use of surfactants for dispersing carbon nanotubes and graphene to make conductive nanocomposites. *Curr. Opin. Colloid Interface Sci.* **2012**, *17*, 225–232. [[CrossRef](#)]
8. Duan, W.H.; Wang, Q.; Collins, F. Dispersion of carbon nanotubes with SDS surfactants: A study from a binding energy perspective. *Chem. Sci.* **2011**, *2*, 1407–1413. [[CrossRef](#)]
9. Vaisman, L.; Wagner, H.D.; Marom, G. The role of surfactants in dispersion of carbon nanotubes. *Adv. Colloid Interface Sci.* **2006**, *128–130*, 37–46. [[CrossRef](#)] [[PubMed](#)]
10. Rashmi, W.; Khalid, M.; Ismail, A.F.; Saidur, R.; Rashid, A.K. Experimental and numerical investigation of heat transfer in CNT nanofluids. *J. Exp. Nanosci.* **2015**, *10*, 545–563. [[CrossRef](#)]
11. Assael, M.J.; Metaxa, I.N.; Arvanitidis, J.; Christofilos, D.; Lioutas, C. Thermal Conductivity Enhancement in Aqueous Suspensions of Carbon Multi-Walled and Double-Walled Nanotubes in the Presence of Two Different Dispersants. *Int. J. Thermophys.* **2005**, *26*, 647–664. [[CrossRef](#)]
12. Aravind, S.S.J.; Baskar, P.; Baby, T.T.; Sabareesh, R.K.; Das, S.; Ramaprabhu, S. Investigation of structural stability, dispersion, viscosity, and conductive heat transfer properties of functionalized carbon nanotube based nanofluids. *J. Phys. Chem. C* **2011**, *115*, 16737–16744. [[CrossRef](#)]
13. Georgakilas, V.; Gournis, D.; Tzitzios, V.; Pasquato, L.; Guldi, D.M.; Prato, M. Decorating carbon nanotubes with metal or semiconductor nanoparticles. *J. Mater. Chem.* **2007**, *17*, 2679–2694. [[CrossRef](#)]
14. Kharisov, B.I.; Kharissova, O.V.; Méndez, U.O.; Fuente, I.G.D. La Decoration of Carbon Nanotubes with Metal Nanoparticles: Recent Trends. *Synth. React. Inorg. Met. Nano-Metal. Chem.* **2016**, *46*, 55–76. [[CrossRef](#)]
15. Sezer, N.; Koç, M. Stabilization of the aqueous dispersion of carbon nanotubes using different approaches. *Therm. Sci. Eng. Prog.* **2018**, *8*, 411–417. [[CrossRef](#)]
16. Cozzarini, L.; Bertolini, G.; Šuran-Brunelli, S.T.; Radivo, A.; Bracamonte, M.V.; Tavagnacco, C.; Goldoni, A. Metal decorated carbon nanotubes for electrocatalytic water splitting. *Int. J. Hydrogen Energy* **2017**, *42*, 18763–18773. [[CrossRef](#)]
17. Duc Chinh, V.; Speranza, G.; Migliaresi, C.; Van Chuc, N.; Minh Tan, V.; Phuong, N.-T. Synthesis of Gold Nanoparticles Decorated with Multiwalled Carbon Nanotubes (Au-MWCNTs) via Cysteaminium Chloride Functionalization. *Sci. Rep.* **2019**, *9*, 5667. [[CrossRef](#)]
18. Guzsvány, V.; Vajdle, O.; Gurdeljević, M.; Kónya, Z. Ag or Au Nanoparticles Decorated Multiwalled Carbon Nanotubes Coated Carbon Paste Electrodes for Amperometric Determination of H₂O₂. *Top. Catal.* **2018**, *61*, 1350–1361. [[CrossRef](#)]
19. Amiri, A.; Shanbedi, M.; Eshghi, H.; Heris, S.Z.; Baniadam, M. Highly Dispersed Multiwalled Carbon Nanotubes Decorated with Ag Nanoparticles in Water and Experimental Investigation of the Thermophysical Properties. *J. Phys. Chem. C* **2012**, *116*, 3369–3375. [[CrossRef](#)]
20. Tang, L.; Duan, F.; Chen, M. Silver nanoparticle decorated polyaniline/multiwalled super-short carbon nanotube nanocomposites for supercapacitor applications. *RSC Adv.* **2016**, *6*, 65012–65019. [[CrossRef](#)]
21. Patole, A.; Lubineau, G. Carbon nanotubes with silver nanoparticle decoration and conductive polymer coating for improving the electrical conductivity of polycarbonate composites. *Carbon N. Y.* **2015**, *81*, 720–730. [[CrossRef](#)]
22. Dinh, N.X.; Van Quy, N.; Huy, T.Q.; Le, A.T. Decoration of silver nanoparticles on multiwalled carbon nanotubes: Antibacterial mechanism and ultrastructural analysis. *J. Nanomater.* **2015**, *16*, 63. [[CrossRef](#)]
23. Markoulidis, F.; Todorova, N.; Grilli, R.; Lekakou, C.; Trapalis, C. Composite Electrodes of Activated Carbon and Multiwall Carbon Nanotubes Decorated with Silver Nanoparticles for High Power Energy Storage. *J. Compos. Sci.* **2019**, *3*, 97. [[CrossRef](#)]

24. Travessa, D.N.; Da Silva, F.S.; Cristovan, F.H.; Jorge, A.M.; Cardoso, K.R. Ag ion decoration for surface modifications of multi-walled carbon nanotubes. *Mater. Res.* **2014**, *17*, 687–693. [[CrossRef](#)]
25. Xin, F.; Li, L. Decoration of carbon nanotubes with silver nanoparticles for advanced CNT/polymer nanocomposites. *Compos. Part. A Appl. Sci. Manuf.* **2011**, *42*, 961–967. [[CrossRef](#)]
26. Cojocaru, A.; Brincoveanu, O.; Pantazi, A.; Balan, D.; Enachescu, M.; Visan, T.; Anicai, L. Electrochemical preparation of Ag nanoparticles involving choline chloride-glycerol deep eutectic solvents. *Bulg. Chem. Commun.* **2017**, *49*, 194–204.
27. Zhou, M.; Zhai, Y.; Dong, S. Electrochemical Sensing and Biosensing Platform Based on Chemically Reduced Graphene Oxide. *Anal. Chem.* **2009**, *81*, 5603–5613. [[CrossRef](#)]
28. Petica, A.; Gavriliu, S.; Lungu, M.; Buruntea, N.; Panzaru, C. Colloidal silver solutions with antimicrobial properties. *Mater. Sci. Eng. B* **2008**, *152*, 22–27. [[CrossRef](#)]
29. Izutsu, K. Fundamentals of Chemistry in Nonaqueous Solutions: Electrochemical Aspects. In *Electrochemistry in Nonaqueous Solutions*; Wiley: Hoboken, NJ, USA, 2009; ISBN 978-3-527-62916-9.
30. Abbott, A.P.; Capper, G.; Davies, D.L.; Munro, H.L.; Rasheed, R.K.; Tambyrajah, V. Preparation of novel, moisture-stable, Lewis-acidic ionic liquids containing quaternary ammonium salts with functional side chains. *Chem. Commun.* **2001**, *19*, 2010–2011. [[CrossRef](#)]
31. Abbott, A.P.; Boothby, D.; Capper, G.; Davies, D.L.; Rasheed, R.K. Deep Eutectic Solvents formed between choline chloride and carboxylic acids: Versatile alternatives to ionic liquids. *J. Am. Chem. Soc.* **2004**, *126*, 9142–9147. [[CrossRef](#)]
32. Zhang, Q.; De Oliveira Vigier, K.; Royer, S.; Jérôme, F. Deep eutectic solvents: Syntheses, properties and applications. *Chem. Soc. Rev.* **2012**, *41*, 7108–7146. [[CrossRef](#)]
33. Koczkur, K.M.; Mourdikoudis, S.; Polavarapu, L.; Skrabalak, S.E. Polyvinylpyrrolidone (PVP) in nanoparticle synthesis. *Dalt. Trans.* **2015**, *44*, 17883–17905. [[CrossRef](#)]
34. Brandão, A.T.S.C.; Rosoiu, S.; Costa, R.; Lazar, O.A.; Silva, A.F.; Anicai, L.; Pereira, C.M.; Enachescu, M. Characterization and electrochemical studies of MWCNTs decorated with Ag nanoparticles through pulse reversed current electrodeposition using a deep eutectic solvent for energy storage applications. *J. Mater. Res. Technol.* **2021**, *15*, 342–359. [[CrossRef](#)]
35. Lee, S.; Choi, S.U.-S.; Li, S.; Eastman, J.A. Measuring Thermal Conductivity of Fluids Containing Oxide Nanoparticles. *J. Heat Transfer* **1999**, *121*, 280–289. [[CrossRef](#)]
36. Wang, X.; Xu, X.; Choi, S.U.S. Thermal Conductivity of Nanoparticle—Fluid Mixture. *J. Thermophys. Heat Transf.* **1999**, *13*, 474–480. [[CrossRef](#)]
37. Timofeeva, E.V.; Routbort, J.L.; Singh, D. Particle shape effects on thermophysical properties of alumina nanofluids. *J. Appl. Phys.* **2009**, *106*, 14304. [[CrossRef](#)]
38. Özerinç, S.; Kakaç, S.; Yazıcıoğlu, A.G. Enhanced thermal conductivity of nanofluids: A state-of-the-art review. *Microfluid. Nanofluid.* **2010**, *8*, 145–170. [[CrossRef](#)]
39. Liu, M.-S.; Ching-Cheng Lin, M.; Huang, I.-T.; Wang, C.-C. Enhancement of thermal conductivity with carbon nanotube for nanofluids. *Int. Commun. Heat Mass Transf.* **2005**, *32*, 1202–1210. [[CrossRef](#)]
40. Yu, W.; Xie, H.; Chen, W. Experimental investigation on thermal conductivity of nanofluids containing graphene oxide nanosheets. *J. Appl. Phys.* **2010**, *107*, 94317. [[CrossRef](#)]
41. Leung, A.B.; Suh, K.I.; Ansari, R.R. Particle-size and velocity measurements in flowing conditions using dynamic light scattering. *Appl. Opt.* **2006**, *45*, 2186–2190. [[CrossRef](#)]
42. Huang, X.; Jain, P.K.; El-Sayed, I.H.; El-Sayed, M.A. Gold nanoparticles: Interesting optical properties and recent applications in cancer diagnostics and therapy. *Nanomedicine* **2007**, *2*, 681–693. [[CrossRef](#)]
43. Khlebtsov, B.N.; Khlebtsov, N.G. On the measurement of gold nanoparticle sizes by the dynamic light scattering method. *Colloid J.* **2011**, *73*, 118–127. [[CrossRef](#)]
44. Tomaszewska, E.; Soliwoda, K.; Kadziola, K.; Tkacz-Szczesna, B.; Celichowski, G.; Cichomski, M.; Szmaja, W.; Grobelny, J. Detection Limits of DLS and UV-Vis Spectroscopy in Characterization of Polydisperse Nanoparticles Colloids. *J. Nanomater.* **2013**, *2013*, 313081. [[CrossRef](#)]
45. Zimbone, M.; Calcagno, L.; Messina, G.; Baeri, P.; Compagnini, G. Dynamic light scattering and UV-vis spectroscopy of gold nanoparticles solution. *Mater. Lett.* **2011**, *65*, 2906–2909. [[CrossRef](#)]
46. Hao, E.; Schatz, G.C.; Hupp, J.T. Synthesis and Optical Properties of Anisotropic Metal Nanoparticles. *J. Fluoresc.* **2004**, *14*, 331–341. [[CrossRef](#)]
47. Bhui, D.K.; Bar, H.; Sarkar, P.; Sahoo, G.P.; De, S.P.; Misra, A. Synthesis and UV-vis spectroscopic study of silver nanoparticles in aqueous SDS solution. *J. Mol. Liq.* **2009**, *145*, 33–37. [[CrossRef](#)]
48. Sato-Berrú, R.; Redón, R.; Vázquez-Olmos, A.; Saniger, J.M. Silver nanoparticles synthesized by direct photoreduction of metal salts. Application in surface-enhanced Raman spectroscopy. *J. Raman Spectrosc.* **2009**, *40*, 376–380. [[CrossRef](#)]
49. Evanoff, D.D.J.; Chumanov, G. Synthesis and optical properties of silver nanoparticles and arrays. *Chemphyschem* **2005**, *6*, 1221–1231. [[CrossRef](#)]
50. Koppel, D.E. Analysis of Macromolecular Polydispersity in Intensity Correlation Spectroscopy: The Method of Cumulants. *J. Chem. Phys.* **1972**, *57*, 4814–4820. [[CrossRef](#)]

51. Brandão, A.T.S.C.; Rosoiu, S.; Costa, R.; Silva, A.F.; Anicai, L.; Enachescu, M.; Pereira, C.M. Characterization of Carbon Nanomaterials Dispersions: Can Metal Decoration of MWCNTs Improve Their Physicochemical Properties? *Nanomaterials* **2022**, *12*, 99. [[CrossRef](#)] [[PubMed](#)]
52. Wang, M.; Li, H.; Li, Y.; Mo, F.; Li, Z.; Chai, R.; Wang, H. Dispersibility and size control of silver nanoparticles with anti-algal potential based on coupling effects of polyvinylpyrrolidone and sodium tripolyphosphate. *Nanomaterials* **2020**, *10*, 1042. [[CrossRef](#)]
53. Yu, J.; Grossiord, N.; Koning, C.E.; Loos, J. Controlling the dispersion of multi-wall carbon nanotubes in aqueous surfactant solution. *Carbon N. Y.* **2007**, *45*, 618–623. [[CrossRef](#)]
54. Li, D.; Müller, M.B.; Gilje, S.; Kaner, R.B.; Wallace, G.G. Processable aqueous dispersions of graphene nanosheets. *Nat. Nanotechnol.* **2008**, *3*, 101–105. [[CrossRef](#)]
55. Pinto, V.V.; Ferreira, M.J.; Silva, R.; Santos, H.A.; Silva, F.; Pereira, C.M. Long time effect on the stability of silver nanoparticles in aqueous medium: Effect of the synthesis and storage conditions. *Colloids Surfaces A Physicochem. Eng. Asp.* **2010**, *364*, 19–25. [[CrossRef](#)]
56. Zhang, B.; Chen, Y.; Wang, J.; Blau, W.J.; Zhuang, X.; He, N. Multi-walled carbon nanotubes covalently functionalized with polyhedral oligomeric silsesquioxanes for optical limiting. *Carbon N. Y.* **2010**, *48*, 1738–1742. [[CrossRef](#)]
57. Yue, L.; Pircheraghi, G.; Monemian, S.A.; Manas-Zloczower, I. Epoxy composites with carbon nanotubes and graphene nanoplatelets—Dispersion and synergy effects. *Carbon N. Y.* **2014**, *78*, 268–278. [[CrossRef](#)]
58. Zhang, X.; Zhang, J.; Quan, J.; Wang, N.; Zhu, Y. Surface-enhanced Raman scattering activities of carbon nanotubes decorated with silver nanoparticles. *Analyst* **2016**, *141*, 5527–5534. [[CrossRef](#)]
59. Li, J.; Liu, C. Ag/Graphene Heterostructures: Synthesis, Characterization and Optical Properties. *Eur. J. Inorg. Chem.* **2010**, *2010*, 1244–1248. [[CrossRef](#)]
60. Paredes, J.I.; Villar-Rodil, S.; Martínez-Alonso, A.; Tascón, J.M.D. Graphene Oxide Dispersions in Organic Solvents. *Langmuir* **2008**, *24*, 10560–10564. [[CrossRef](#)]
61. Saion, E.; Gharibshahi, E.; Naghavi, K. Size-controlled and optical properties of monodispersed silver nanoparticles synthesized by the radiolytic reduction method. *Int. J. Mol. Sci.* **2013**, *14*, 7880–7896. [[CrossRef](#)]
62. Singaravelan, R.; Bangaru Sudarsan Alwar, S. Electrochemical synthesis, characterisation and phytogetic properties of silver nanoparticles. *Appl. Nanosci.* **2015**, *5*, 983–991. [[CrossRef](#)]
63. Chen, S.; Wei, Y.; Zou, L.; Lu, H.; Xu, Y.; Hua, J.; Sun, H.; Peng, X.; Liu, B. Preparation and characterization of multi-walled carbon nanotubes decorated with silver nanoparticles through ultraviolet irradiation reduction. *Appl. Organomet. Chem.* **2017**, *31*, 1–7. [[CrossRef](#)]
64. Nagajyothi, P.C.; Veeranjanya Reddy, L.; Devarayapalli, K.C.; Prabhakar Vattikuti, S.V.; Wee, Y.J.; Shim, J. Environmentally Friendly Synthesis: Photocatalytic Dye Degradation and Bacteria Inactivation Using Ag/f-MWCNTs Composite. *J. Clust. Sci.* **2021**, *32*, 711–718. [[CrossRef](#)]
65. Cheng, X.; Zhong, J.; Meng, J.; Yang, J.; Jia, F.; Xu, Z.; Kong, H.; Xu, H. Characterization of Multiwalled Carbon Nanotubes Dispersing in Water and Association with Biological Effects. *J. Nanomater.* **2011**, *2011*, 938491. [[CrossRef](#)]
66. Li, H.; Qiu, Y. Dispersion, sedimentation and aggregation of multi-walled carbon nanotubes as affected by single and binary mixed surfactants. *R. Soc. Open Sci.* **2019**, *6*, 190241. [[CrossRef](#)]
67. Kausar, A.; Siddiq, M. Carbon nanotubes/silver nanoparticles/poly(azo-thiourea) hybrids: Morphological, tensile and conductivity profile. *J. Compos. Mater.* **2014**, *48*, 3271–3280. [[CrossRef](#)]
68. Zaib, Q.; Adeyemi, I.; Warsinger, D.M.; AlNashef, I.M. Deep Eutectic Solvent Assisted Dispersion of Carbon Nanotubes in Water. *Front. Chem.* **2020**, *8*, 1–14. [[CrossRef](#)]
69. Eaton, P.; Quaresma, P.; Soares, C.; Neves, C.; de Almeida, M.P.; Pereira, E.; West, P. A direct comparison of experimental methods to measure dimensions of synthetic nanoparticles. *Ultramicroscopy* **2017**, *182*, 179–190. [[CrossRef](#)]
70. Slistan-Grijalva, A.; Herrera-Urbina, R.; Rivas-Silva, J.F.; Ávalos-Borja, M.; Castellón-Barraza, F.F.; Posada-Amarillas, A. Synthesis of silver nanoparticles in a polyvinylpyrrolidone (PVP) paste, and their optical properties in a film and in ethylene glycol. *Mater. Res. Bull.* **2008**, *43*, 90–96. [[CrossRef](#)]
71. Singh, A.K.; Raykar, V.S. Microwave synthesis of silver nanofluids with polyvinylpyrrolidone (PVP) and their transport properties. *Colloid Polym. Sci.* **2008**, *286*, 1667–1673. [[CrossRef](#)]
72. Hatt, J.W.; Germain, E.; Judd, S.J. Granular activated carbon for removal of organic matter and turbidity from secondary wastewater. *Water Sci. Technol. A J. Int. Assoc. Water Pollut. Res.* **2013**, *67*, 846–853. [[CrossRef](#)]